Mol Neurobiol (2011) 44:111–121
DOI 10.1007/s12035-011-8194-0

Progressive Myoclonic Epilepsy-Associated Gene KCTD7 is a Regulator of Potassium Conductance in Neurons

Régis Azizieh · David Orduz · Patrick Van Bogaert · Tristan Bouschet · Wendy Rodriguez · Serge N. Schiffmann · Isabelle Pirson · Marc J. Abramowicz

Received: 18 April 2011 / Accepted: 13 June 2011 / Published online: 28 June 2011

Abstract The potassium channel tetramerization domain-containing protein 7 (KCTD7) was named after the structural homology of its predicted N-terminal broad complex, tramtrack and bric à brac/poxvirus and zinc finger domain with the T1 domain of the Kv potassium channel, but its expression profile and cellular function are still largely unknown. We have recently reported a homozygous nonsense mutation of *KCTD7* in patients with a novel form of autosomal recessive progressive myoclonic epilepsy. Here, we show that KCTD7 expression hyperpolarizes the cell membrane and reduces the excitability of transfected neurons in patch clamp experiments. We found the expression of KCTD7 in the hippocampal and Purkinje cells of the murine brain, an expression profile consistent with our patients' phenotype. The effect on the plasma membrane resting potential is possibly mediated by Cullin-3, as we demonstrated direct molecular interaction of KCTD7 with Cullin-3 in co-immunoprecipitation assays. Our data link progressive myoclonic epilepsy to an inherited defect of the neuron plasma membrane's resting potential in the brain.

Keywords KCTD7 · Cullin-3 · Potassium channel · Progressive myoclonic epilepsy · EPM3

R. Azizieh (✉) · T. Bouschet · W. Rodriguez · I. Pirson · M. J. Abramowicz
Institute of Interdisciplinary Research (IRIBHM)-ULB, Brussels, Belgium
e-mail: regismanga@gmail.com

I. Pirson
e-mail: ilpirson@ulb.ac.be

M. J. Abramowicz
Department of Medical Genetics, Hôpital Erasme–ULB, Brussels, Belgium

D. Orduz · S. N. Schiffmann
Laboratory of Neurophysiology-ULB, Brussels, Belgium

P. Van Bogaert
Department of Pediatric Neurology, Hôpital Erasme–ULB, Brussels, Belgium

I. Pirson
Institute of Interdisciplinary Research, IRIBHM, School of Medicine, Free University of Brussels (ULB), Campus Erasme, Building C, 808, Route de Lennik, 1070 Brussels, Belgium

Introduction

The potassium channel tetramerization domain-containing protein 7 (KCTD7) belongs to a family of proteins named after the homology of their conserved N-terminal broad complex, tramtrack and bric à brac/poxvirus and zinc finger (BTB/POZ) domain with the T1 domain of the voltage-gated potassium channel (Kv) that allows its tetramerization [1]. We recently observed a biallelic nonsense mutation of the *KCTD7* gene in patients with a familial, autosomal recessive form of progressive myoclonic epilepsy (PME) [2]. PME is characterized by myoclonic epilepsy and progressive neurological dysfunction, mainly ataxia and dementia [3]. Causes of PME include lysosomal storage diseases, mitochondrial encephalopathies and system degeneration diseases (e.g. Unverricht-Lundborg disease). Mutations in ion channels, disturbing transmembrane current conduction and membrane potential have not yet been reported in PME, unlike in other forms of generalized epilepsy, e.g. mutations of potassium channel subunits KCNQ2 [4] and KCNQ3 [5] in familial benign neonatal convulsions.

Little is known about *KCTD7*. Its cDNA was isolated in systematic efforts at characterizing full-length cDNA clones from several libraries [6]. Although *KCTD7*-expressed sequence tags were found in brain tissue samples, the pattern of tissue expression and the cellular function of KCTD7 are largely unknown. The KCTD7 protein consists of 289 amino acids, where the BTB/POZ domain encompasses residues 48 through 104 [7]. Sequence comparison shows that KCTD7 is extremely conserved across species [99% amino acid conservation between human and chimpanzee (*Pan troglodytes*), 97% between human and mouse (*Mus musculus*)], especially at the level of the BTB/POZ domain. KCTD7 is much smaller than a typical potassium channel subunit, and its computed hydrophobicity profile does not indicate a transmembrane segment. It is hence extremely unlikely that KCTD7 would function as a transmembrane channel for potassium or other ions, although an interaction with a potassium channel, especially via their respective BTB/POZ domains, is a possible working hypothesis. Other hypotheses on KCTD7 function are numerous, however, as members of the KCTD family have been involved in a range of various cellular functions, e.g. the modulation of Wnt/beta catenin signaling by KCTD15 [8] or the degradation of histone deacetylase HDAC1 via an E3 ubiquitin ligase complex formed by KCTD11 and Cullin-3 [9]. Here, we studied the expression profile and cellular function of KCTD7 in an effort to understand the pathological mechanism leading to progressive myoclonic epilepsy in our previously reported family.

Materials and Methods

Reagents, antibodies and plasmids Cycloheximide and Nonidet P-40 were purchased from Calbiochem. Anti-Flag monoclonal antibody (M2, Sigma), anti-HIS monoclonal antibody (BD Transduction Laboratories), anti-HA monoclonal antibody (Roche Diagnostics), anti-KCTD7 rabbit polyclonal antibody (ABCam), anti-KCTD7 rabbit monoclonal antibody (Aviva), anti-KCTD7 mouse polyclonal antibody (Abnova), anti-CTIP2 rat polyclonal antibody (Abcam), anti-calbindin rabbit polyclonal antibody (Abcam), anti-iodized thyroglobulin rabbit antibody (Dako) and the donkey monoclonal anti-mouse secondary antibodies (Jackson Immuno Research Europe) were obtained commercially. Lipofectamine 2000 and Dynabeads mRNA purification kit were purchased from Invitrogen, Fugene 6 from Roche Diagnostics, poly-D-lysine, laminin from BD Bioscience, protein G-Sepharose for immunoprecipitation from GE Healthcare, Ribonucleosides Triphosphate Set from Roche and pBluescript II from Stratagene.

Full-length KCTD7 cDNA obtained from mouse brain samples was amplified using the Pfx DNA polymerase (Invitrogen) and cloned respectively in pCIG2-GFP (generous gift by Franck Polleux), pAcGFP-N1 (Clontech), pcDNA3-HISa and pcDNA3-HA (Invitrogen) vectors. pEF-HA Cullin1 and pEF-HA Cullin-3 were kind gifts from Dr A. Andrés (CSIC University of Valladolid, Spain). Flag-ubiquitin was received from Dr. Wallace Y. Langdon (University of Western Australia). The primers used for KCTD7 amplification were: 5′-TAGCCTCGAGCACCGCCCAGAGCCAGAG and TAGCCTGCAGTCACCACCACGTGATTTTGAACTC-3′ for XhoI and PstI cloning in pCIG2 GFP; 5′-TAGCGAATTC ACCGCCCAGAGCCAGAG and TAGCGGATCCCAC CACCACGTGATTTTGAACTC-3′ for EcoRI and BamHI cloning in pACGFPN; 5′-TAGCGGATCCCACCGCCCAG AGCCAGAG and TAGCCTTAAGTCACCACCACGTGA TTTTGAACTC-3′ for BamHI and EcoRI cloning in pcDNA3-HISa; and 5′-TAGCGGATCCCCGCCCAGAGCC AGAGGG and TAGCCTTAAGTCACCACCACGT GATTTTGAACTC-3′ for BamHI and EcoRI cloning in pcDNA3 HA.

Cell culture and transfection conditions COS-7 were cultured in Dulbecco's modified Eagle's medium (Invitrogen) supplemented with 10% foetal bovine serum (Gibco, Invitrogen), 100 U/ml penicillin (Invitrogen), 100 μg/ml streptomycin (Invitrogen), 2.5 μg/ml fungizone (Invitrogen) and 2 mM Na pyruvate (Gibco, Invitrogen). Mice embryos E13.5 were dissected in Leibovitz's 15 medium (Gibco, Invitrogen) supplemented with glucose 1 M. Progenitor neurons were cultured in neurobasal medium (Gibco, Invitrogen) supplemented with B27 (Gibco, Invitrogen), 100 U/ml penicillin (Invitrogen), 100 μg/ml streptomycin (Invitrogen), 2.5 μl/ml fungizone (Invitrogen) and 0.5% L-glutamine. These embryonic neurons were cultured 24 h on poly-D-lysine and laminin-coated coverslips in 12 well plates. Cells were grown at 37°C in a 5% CO_2-humidified atmosphere. COS-7 cells were plated at 1×10^6 cells/10 cm dish and embryonic neurons at 5×10^5/well (in a 12 well plate) the day before transfection. We transfected COS cells with 4 μg of DNA for each construct: GFP-, HIS- or HA-tagged KCTD7, HA-Cullin1 or 3 and Flag-ubiquitin using Fugene 6 according to the manufacturer's instructions (Roche Diagnostics). We transfected embryonic neurons with 10 μg of DNA using Lipofectamine 2000 according to the manufacturer's instructions (Invitrogen).

Electrophysiology Dishes with primary cultured cortical neurons (10–15 days in culture) were used for electrophysiological recordings. The dishes were installed in a recording chamber and submerged in a continuously flowing bicarbonate-buffered saline [125 mM NaCl, 2.5 mM KCl, 1.25 mM NaH_2PO_4, 26 mM $NaHCO_3$, 2 mM $CaCl_2$, 1 mM $MgCl_2$ and 10 mM glucose equilibrated with a 95%O_2–5%CO_2 mixture (pH 7.3)] at 22–24°C with a 1.5 ml/min flux rate. GFP-expressing

cortical neurons were visualized with a ×63 water immersion objective placed in a Zeiss upright microscope (Axioskop 2FS Plus, Zeiss, Oberkochen, Germany) and identified with a mercury UV lamp (Zeiss, HBO 50/AC) and a FITC filter (excitation BP 450/490, beam splitter FT 510 and emission LP 515). The selected cells were then recorded using the whole cell configuration of the patch-clamp technique with a double EPC-10 operational amplifier (HEKA Elektronik, Lambrecht/Pfalz, Germany). Patch pipettes were made from borosilicate glass capillaries (Hilgenberg GmbH, Malsfeld, Germany) with a two-stage vertical puller (PIP 5, Heka Elektronik, Lambrecht/Pfalz, Germany) and filled with an internal solution containing: 119 mM $KMeSO_4$, 1 mM $MgCl_2$, 0.1 mM $CaCl_2$, 10 mM HEPES, 1 mM EGTA, 12 mM phosphocreatine, 2 mM Na_2ATP and 0.7 mM Na_2GTP adjusted to a of pH 7.2–3 with 1 M KOH and an osmolarity of 280–300 mOsm/l. Pipette input resistances were in the 4.5–6.5 MΩ range. Tight gigaohm seals (>2 GΩ) were obtained before the rupture of the membrane patch. The holding potential was maintained at −70 mV and 2 min were respected before the beginning of the recordings. Subsequent hyperpolarizing pulses of −10 mV were applied to extract the passive cellular parameters by analyzing the elicited current transients [10]. Thus, series resistance, membrane capacitance and input resistance were monitored during the entire experiment. Experiments with series resistance values >30 MΩ were discarded. Voltage clamp and current clamp recordings were filtered at 10 kHz and then digitized at 20 kHz by using the acquisition software Patchmaster (HEKA, Lambrecht/Pfalz, Germany). Cellular capacitances were monitored on both groups: 62.62±6.04 and 40.55±4.69 pF for control GFP and overexpressing KCTD7 neurons, respectively ($p \leq 0.05$). Data analyses were performed using the Neuromatic software package (www.neuromatic.thinkrandom.com) and custom routines within the IgorPro environment (Wavemetrics, Lake Oswego, OR, USA). All values are expressed as mean±SEM and all statistical tests were performed using Student's *t* test within Excel software package (Microsoft). The significance level was established at $p<0.05$ (*).

Immunoprecipitation and immunoblotting Forty-eight hours after transfection, COS-7 cells were washed twice with ice cold phosphate-buffered saline (PBS) and harvested in 500 µl of lysis buffer (80 mM Tris–HCl pH 7.5, 150 mM NaCl, 20 mM EDTA, 200 mM NaF, 1% Brij, 4 mM sodium orthovanadate, 5 mM $Na_4P_2O_7$, 1 µM okadaic acid and a mix of protease inhibitors Complete (Roche Diagnostics). Lysis was allowed to continue for 60 min at 4°C. The cell lysates were clarified by centrifugation at 13,000 rpm for 10 min at 4°C and the protein concentration was measured using the Bradford method [36???]. Fifty micrograms of the whole cell lysis was tested by immunoblot to verify protein expression. Cells lysates were precleared with protein G-Sepharose at 4°C for 60 min and then incubated with antibody-bound protein G-Sepharose for 3 h at 4°C. The beads were washed three times with lysis buffer containing protease inhibitors and two times with lysis buffer without inhibitors. Proteins were separated by SDS-PAGE, transferred onto nitrocellulose membranes and immunoblotted using appropriate antibodies. Proteins on the membranes were then revealed using Odyssey Infrared Imaging System (LI-COR Biosciences).

Immunofluorescence COS-7 cells were seeded on coverslips in 12 well plates at 3×10^5 cells/well in the supplemented Dulbecco's modified Eagle's medium as described above and transfected 24 h later. Forty-eight hours after transfection, the cells were washed twice with PBS, fixed with 4% paraformaldehyde (Sigma) for 15 min at room temperature, washed again twice with PBS, incubated for 5 min with 0.2% Triton, washed once with PBS, incubated with $NaBH_4$ 5 min, washed once with PBS and incubated with the primary antibody solution (1:500 dilution) for 2 h on a table. The coverslips were then washed three times with PBS and incubated with the secondary antibody (1:10,000) for an hour preserved from light. Coverslips were then washed three times with PBS, incubated with DAPI, washed three times with PBS, rinsed with water and fixed with glycergel (Invitrogen). Finally, the cells were observed in fluorescence microscopy using a Zeiss Axioplan 2 Imaging microscope (Zeiss) with a blue laser diode (475 nm) and in confoncal microscopy using a Zeiss Axio CSM 700 (Zeiss) with blue laser diode (475 nm).

RNA extraction and RT-PCR Mouse tissues were lysed in Tri-Reagent (Ambion) and centrifuged 10 min at 13,000 rpm at 4°C. Two hundred microlitres of Rnase-free chloroform (VWR Prolabo) were added to the supernatant. Each sample was then centrifuged at 13,000 rpm for 15 min at 4°C. One volume of ice cold 70% ethanol was then added to the supernatant. Each sample was then purified on RNeasy columns (Qiagen) according to the manufacturer's instructions. Once purified, 2.5 µl of the RNA samples were subjected to reverse transcription using the Super-Script II Reverse Transcriptase kit (Invitrogen) following the manual's instructions. Once all the samples were reverse transcribed, 50 ng of template cDNA was engaged in "touch down" PCR: initial denaturation at 94°C for 2 min and 30 s, 20 cycles including denaturation at 94°C, hybridization at 62°C to 52°C (−0.5°C each cycle) and elongation at 72°C, followed by 20 other cycles at constant 52°C melting temperature.

Northern blotting mRNA were purified from total RNA samples by hybridization on Dynabead (Invitrogen) according

to the manufacturer's instruction. The mRNA samples were then denatured 1 h at 50°C and separated by electrophoresis on a 1% agarose gel. mRNA were transferred during 8 h on a nylon membrane on a bridge humidified by 20x SSC (3 M NaCl and 0.3 M trisodium citrate) and samples were then fixed on the membrane heating 2 h at 80°C. The membrane was prehybridized for 4 h at 42°C in hybridization solution (formamide 50%, 5x SSPE, 5x Denhardt, 0.3% SDS, sperm DNA 250 μg/ml and bovine serum albumin 200 μg/ml). The KCTD7-specific probe was designed by PCR (5′-TCGAAT GAGTAGGACTTGGTG and CCGCATCTTAATA ACAATTCAG-3′) and labelled by ^{32}P using the Megaprime DNA Labelling System (GE Healthcare, Amersham) according to the manufacturer's instructions and denatured 10 min at 100°C before use. The radioactive probe was added to the hybridization solution supplemented with dextran sulphate sodium salt (Sigma), and the membrane was hybridized over night at 42°C before being washed twice at room temperature in 2x SSC 0.1% SDS, and four times at 65°C in 0.1xSSC 0.1% SDS. The membrane was finally revealed by autoradiography using Amersham Hyperfilm (GE Healthcare, Amersham).

In situ hybridization CD1 mice were sacrificed and perfused with RNase free 4% paraformaldehyde (Sigma). Brains were extracted and immerged overnight in 4% paraformaldehyde. The next day, the brains were immerged overnight in 20% sucrose and the day after, overnight in 30% sucrose. Finally, brains were included in O.C.T. (Tissue-Tek) and cut on using a cryostat at 20 μm. Riboprobes (anti-sense and sense) were expressed with the Ribonucleosides Triphosphate Set (Roche) and T3/7 RNA polymerase (Roche) from the whole coding sequence of KCTD7 cDNA cloned in pBluescript II (Stratagene). The brain slices were fixed first time 15 min in 4% paraformaldehyde, washed once with RNAse free water and twice with 1x PBS 0.1% Tween20 (Sigma). They were then immerged 2 min in 6% H_2O_2–1x PBS 0.1% Tween20 and washed three times 5 min in 1x PBS 0.1% Tween20. Each slice was then treated 1 min with proteinase K (1 μg/ml) in 1x PBS 0.1% Tween20 and washed for 10 min in glycine (2 mg/ml)–1x PBS 0.1% Tween20 and three times for 5 min in 1x PBS 0.1% Tween20. Slices were then fixed 15 min in 4% paraformaldehyde–0.2% glutaraldehyde, washed three times for 5 min in 1x PBS 0.1% Tween20 and incubated with the prehybridization solution for 1 h at 70°C. The riboprobes (anti-sense and sense) were incubated 2 min at 80°C for denaturation and added to the prehybridization solution overnight at 70°C. The next day, the brain slices were washed three times for 15 min in 1x SDS–formamide 50%–SSC, three times for 15 min formamide50%–SSC, and three times 15 min in TBS 0.1% Tween20 5% before being blocked with TBS 0.1%–Tween20 5%–lamb serum 1 h at room temperature. All slices were then incubated over night with 1/2,000 anti-digoxigenin (Roche) in TBS 0.1%–Tween20 5%–lamb serum. The next day, the brain slices were washed four times for 15 min in TBS 0.1% Tween20 and three times 10 min NaCl (100 mM) Tris–HCl (100 mM)–Tween20 (0.1%)–$MgCl_2$ (50 mM). All slices were then incubated with the revelation signal. The last day, the brain slices were washed for 10 min in 1x PBS–20 mM EDTA pH 8, fixed for 20 min in 4% paraformaldehyde, washed two times for 10 min in 1x PBS, and dehydrated for 2 min in 70% ethanol, 2 min in 90% ethanol, 30 s in 100% ethanol and finally mounted. Finally, the slices were examined in optical microscopy using a Zeiss Axioplan 2 Imaging microscope (Zeiss).

Immunohistochemistry New brain slices cut at 20 μm were defrozen for 10 min on the bench, dried out for 10 min in acetone, dried for 10 min on the bench and rehydrated for 30 min in 1x PBS–1% BSA always at room temperature. All slices were then washed twice in 1x PBS, twice in water and denatured at 98°C (epitope retrieval) using a PT module (LabVision). The brain slices were treated 20 min in 1% H_2O_2 to suppress the endogenous peroxydase activity, washed twice in water, blocked 1 h in 1x PBS–1% BSA–2% donkey serum and incubated overnight with the primary antibody (1/250) in 1x PBS–1% BSA–2% donkey serum. The next day, all slices were washed three times for 2 min in 1x PBS, incubated with the secondary antibody (1/250) 1 h at room temperature, washed three times for 2 min in 1x PBS, incubated with Vectastain ABC system (Vector) for 30 min at room temperature, washed three times in 1x PBS and finally revealed with diaminobenzidine (Dako). At last, the slices were examined in optical microscopy using a Zeiss Axioplan 2 Imaging microscope (Zeiss).

Results

KCTD7 Decreases Excitability of Cultured Cortical Neurons

To evaluate the possible influence of KCTD7 on neuronal excitability, electrophysiological recordings were performed on primary cultures of cortical neurons obtained from E13.5 murine embryo cortical neurons, transfected with a bicistronic expression vector expressing either the green fluorescent protein (GFP) only (control) or GFP and KCTD7, by using the whole cell configuration of the patch clamp technique. Intrinsic excitability was studied in current clamp recordings by setting membrane potential at −70 mVand injecting 200 ms steps of depolarizing current from 0 to 380 pA, by 20 pA increments. With this protocol, we found that neurons over-expressing KCTD7 (n=12) presented higher threshold

currents to elicit a first action potential than control GFP neurons (n=14): 63.63±5.95 and 42.22±6.82 pA, respectively. As depicted in Fig. 1, the same amount of current that succeeds to evoke a burst of action potential in control GFP neurons (Fig.1, a1) is a subthreshold current for overexpressing KCTD7 neurons (Fig. 1, a2). On the other hand, as determined in voltage clamp experiments, membrane resistance values (Fig.1, b1) were smaller in neurons overexpressing the KCTD7 protein (0.87±0.17 GΩ) as compared to the control GFP group (1.42±0.19 GΩ). Furthermore, the resting potential for the group of neurons overexpressing the KCTD7 protein was clearly hyperpolarized (−65.27± 1.69 mV) with respect to the control GFP group (−54.02± 3.48 mV) (Fig. 1, b2).

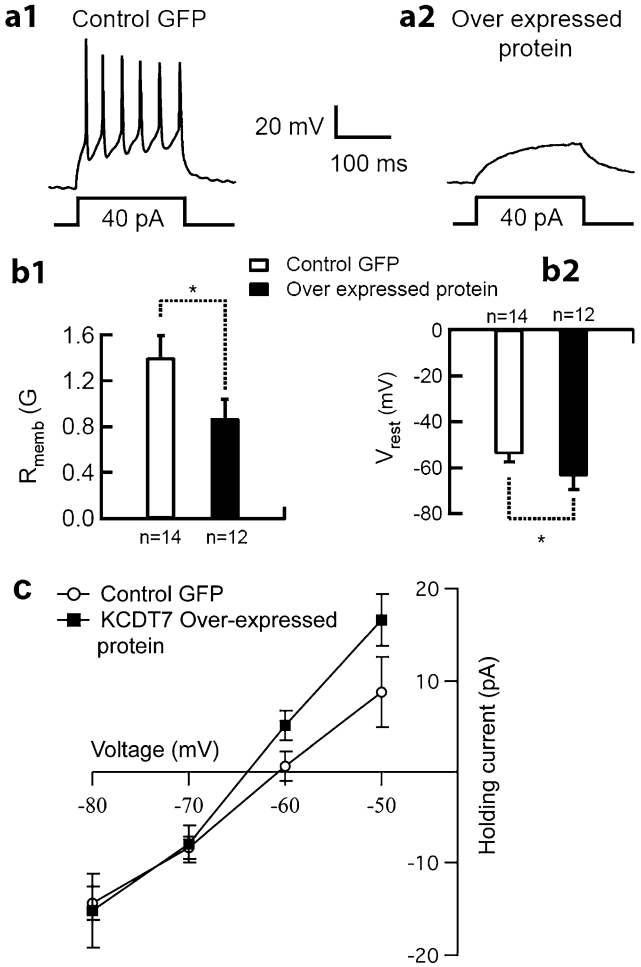

Fig. 1 *KCTD7* overexpression decreases the excitability of cortical primary neurons. **a1** A suprathreshold current pulse (200 ms, duration; 40 pA, amplitude) induces a 30-Hz firing pattern on a control GFP pyramidal neurone in culture. **a2** By contrast, the same current pulse is unable to induce any action potential on KCTD-overexpressing neurons. **b1–b2** Pooled values (mean±SEM) for membrane resistance (R_{memb}) and resting potential (V_{rest}) measured from control GFP (*white columns*) and overexpressing KCTD7 (*black columns*) cortical neurons in culture. R_{memb} is smaller and V_{rest} is more negative in KCTD7-overexpressing neurons compared to control GFP neurons. The *bars* denote the SEM. *$p \leq 0.05$, Student's t test. **c** I/V plots for both controls and KCTD7-overexpressing cells. For the KCDT7-overexpressing group (n=6), the I/V plot crossed the zero voltage at a more hyperpolarized value compared to the controls (n=6)

From voltage clamp experiments, we extracted the holding current values for voltages between −80 to −50 mV. Interestingly, the curves followed the tendency of the resting potentials measured in the current clamp configuration (Fig. 1c). For the KCDT7 protein overexpressing group of cells (n=6), the I/V plot crossed the zero voltage at a more hyperpolarized value compared to controls (n=6). This value was near the value measured previously in current clamp experiments (−65.27 mV). For the GFP control group, this reverse point was more depolarized.

KCTD7 is Expressed in the Mitral Cells of the Olfactory Bulbs, the Hippocampus, the Deep Layers of the Cerebral Cortex and Purkinje Cells of the Cerebellum

To investigate the tissue expression of *KCTD7*, we first performed a Northern blot analysis of mRNA samples extracted from brain, heart, liver, lung, intestine, colon, kidney, spleen, eye and muscle of CD1 mice (Fig. 2a). Blots were exposed to radio-labelled cDNA probes of *KCTD7* or GADPH used as a control. We observed a robust KCTD7 mRNA signal in each tissue tested. To confirm these results, an RT-PCR assay targeting exon 1 to 3 of *KCTD7* was performed on several mRNA samples of CD1 mice (Fig. 2b). Consistent with the Northern blot results, a cDNA fragment of expected size was amplified in every tissue tested.

In order to clarify whether the *KCTD7* transcript had a specific distribution in the brain we preformed in situ hybridization of anti-sense and sense riboprobes covering the whole coding sequence of the *KCTD7* cDNA. This showed a strong signal in the mitral cells of the olfactory bulb (data not shown), the dentate gyrus and CA1-CA3 hippocampal cells, the deep layers of the cerebral cortex and the Purkinje cells of the cerebellum (Fig. 3a).

Considering that KCTD 7 protein sequence is 97% conserved between human and mouse, we purchased a commercial polyclonal rabbit antibody against human KCTD7 from Abcam. We confirmed its specificity by Western blotting of protein extracts from COS-7 cells transfected with native, or HIS-tagged human KCTD7 cDNA constructs, using both the anti-KCTD7 and the anti HIS-tag and HA-tag antibodies (Fig. 4a).

Protein extracts from various mouse tissues (brain, heart, lungs, liver, kidney, pancreas, stomach, intestine and colon) failed to produce a specific signal in Western blotting experiments using three different antibodies against KCTD7 (Abcam, Abnova and Aviva). This was true for adult mouse tissue extracts as well as for E6 to E14 embryonic tissues (data not shown). We did, however, readily detected the recombinant protein with either the

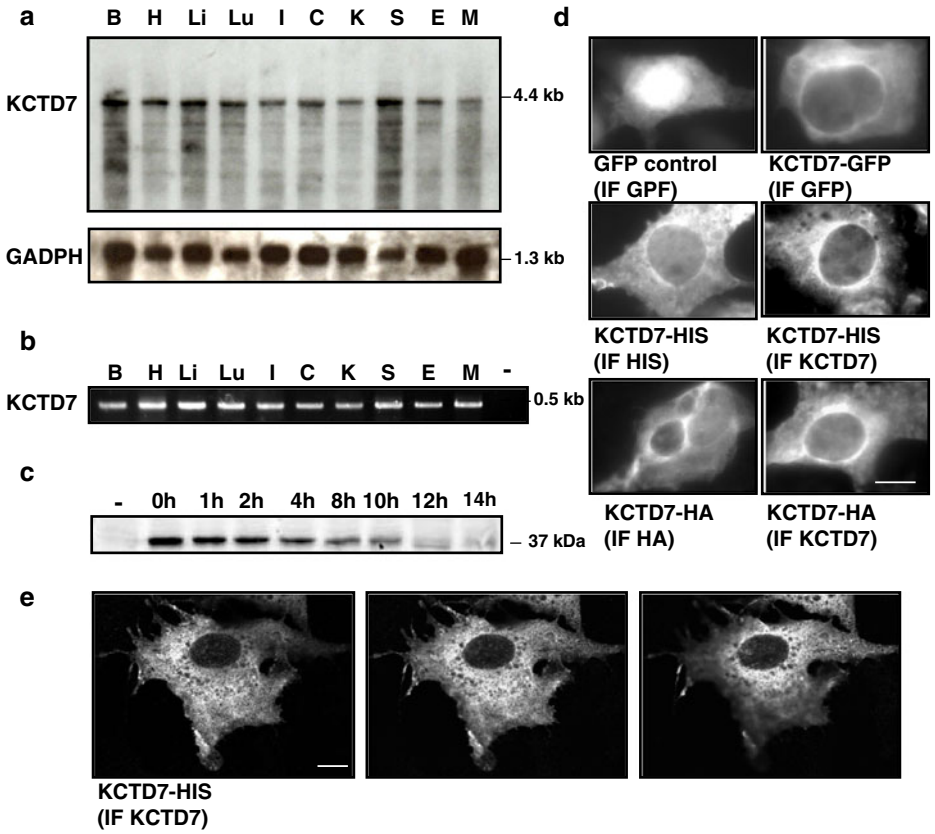

Fig. 2 *KCTD7* expression. **a** Northern blotting of mRNAs purified from adult mouse brain (*B*), heart (*H*), liver (*Li*), lung (*Lu*), intestine (*I*), colon (*C*), kidney (*K*), spleen (*S*), eye (*E*) and muscle (*M*), probed by a full-length KCTD7 cDNA. GADPH cDNA was used as control of mRNA samples. **b** RT-PCR amplification of segments 1 to 493 of KCTD7 mRNA in the same tissues; brain (*B*), heart (*H*), liver (*Li*), lung (*Lu*), intestine (*I*), colon (*C*), kidney (*K*), spleen (*S*), eye (*E*) and muscle (*M*); (*hyphen*) H20 instead of mRNA. **c** Western blotting of protein extracts from COS-7 cells transfected with KCTD7 cloned in pCIG2GFP. Cells were harvested at various times after protein synthesis inhibition by cycloheximid (10 μg/μl), indicating a protein half-life of approximately 6 h and complete disappearance of the signal after 14 h. **d** Immunofluorescence on COS-7 expressing various KCTD7 constructs and tested with anti-GFP, anti-HIS, anti-HA or anti-KCTD7 antibodies as described. *Scale bar*=10 μm. **e** Immunofluorescence in confocal microscopy on COS-7-expressing HIS-KCTD7 and detected with anti-KCTD7 antibodies. *Scale bar*=10 μm

KCTD7 or the Tag antibody Our ISH and immunohistochemistry data showed that KCTD7 is expressed a specific subgroup of cells, explaining maybe why the protein is present at too low level to be properly detectable in protein samples.

In view of the contrast between strong, ubiquitous mRNA detection by Northern blotting and absent signal in Western blotting experiments, we hypothesized that KCTD7 might be a very labile protein. We used cyclohemixide, an inhibitor of protein synthesis interfering with the translational elongation, as a tool to measure the stability of recombinant KCTD7. We transfected KCTD7 in a COS-7 cell line and added cycloheximid 24 h later. Cells were harvested at indicated times (Fig. 2c). KCTD7 was detected in all samples by Western blotting using a specific KCTD7 antibody (Abnova). As shown in Fig. 2c, KCTD7 is not a labile protein. It showed a half-life of 6 h and the signal disappeared after 14 h. Furthermore, we confirmed that the endogenous protein could not be detected upon treatment of the cells with MG132, a proteasome inhibitor that mediates the degradation of ubiquitin-conjugated proteins in mammalian cells. We cultured COS-7 cells and SHY5Y cells and added MG132 (10 μM). Cells were harvested at 0, 6, 12 or 24 h after the treatment and the extracts were analyzed by Western blot using KTD7 antibodies. We failed to detect intracellular KCTD7 protein after the addition of MG132 (data not shown).

We then used immunohistochemistry to detect the KCTD7 protein in specific cells in coronal slices of a P30 CD1 murine brain using the KCTD7 rabbit polyclonal antibody (Abcam). In perfect correspondence with mRNA in situ hybridization, we observed a KCTD7 protein signal in mitral cells of the olfactory bulb (data not shown), the dentate gyrus and CA1-CA3 cells of the hippocampus, the deep layers of the cerebral cortex and the Purkinje cell layer of the cerebellum (Fig. 3b). Anti-thyroglobulin antibodies were used during the experiments as a negative control (Fig. 3b). In addition, anti-CTIP2 antibodies were used as a positive control for the hippocampus as well as anti-Calbindin antibodies for the Purkinje cell layer (Fig. 3c).

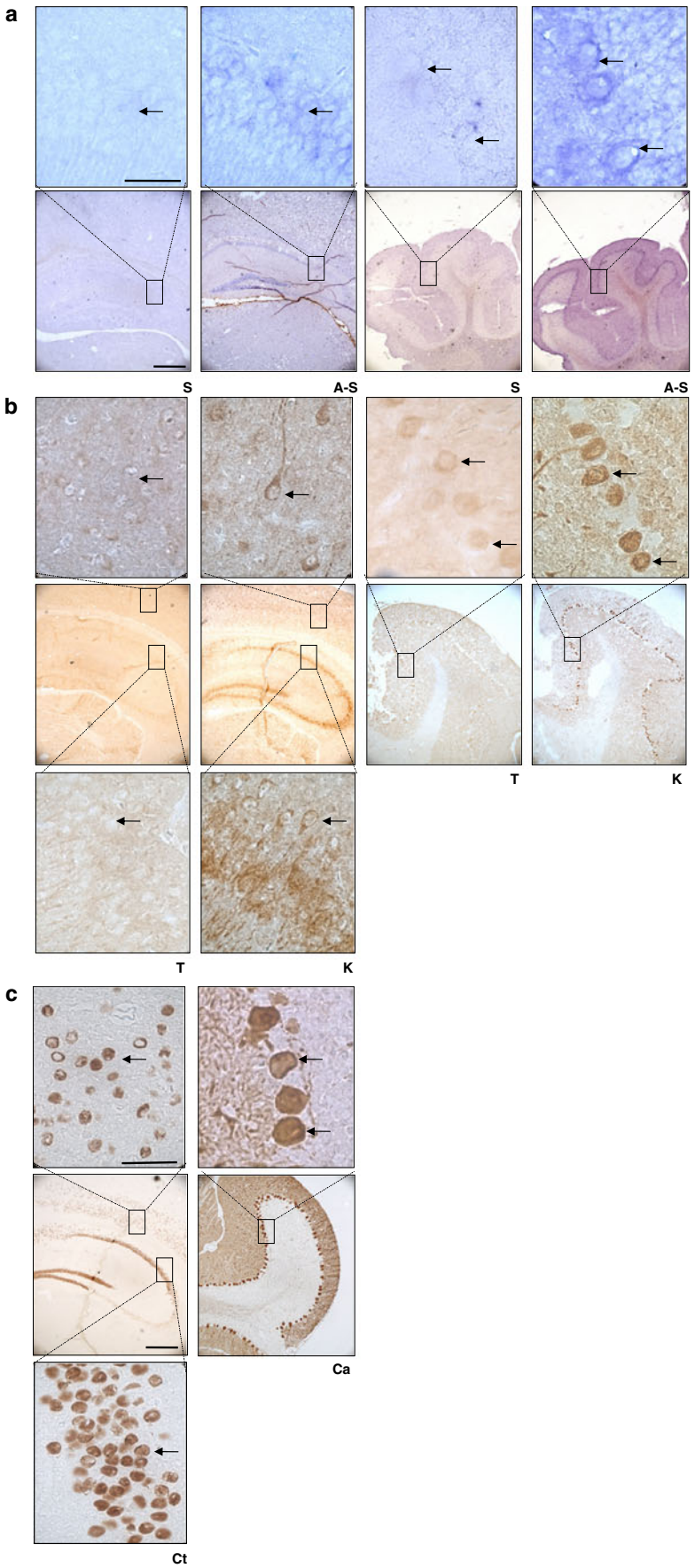

Fig. 3 *KCTD7* transcript and protein in murine brain. **a** In situ hybridization of brain coronal slices from adult mouse brain (P30) using anti-sense (*A-S*) KCTD7 riboprobes and sense (*S*) KCTD7 riboprobes as a negative control, shown on the *left side*, the cerebral cortex and the hippocampus and on the *right side*, the cerebellum. *Scale bar*= 70 μm (*above*) and 500 μm (*below*). **b** Immunohistochemistry using an anti-KCTD7 antibody (*K*) and an anti-iodized thyroglobulin antibody (*T*) as a negative control in the same regions of the brain as for in situ hybridization, showing staining of hippocampal neurons (*arrows*) and cerebral cortex neurones (*arrows*) on the left side, and the Purkinje cell layer (*arrows*) on the right side. *Scale bar*=70 μm (*above*) and 500 μm (*below*). **c** Complementary immunohistochemistry using an anti-CTIP2 antibody (*Ct*) as a positive control for the hippocampus on the left side, hippocampal neurons (*arrows*) and cerebral cortex neurones (*arrows*)and an anti-Calbindin antibody (*Ca*) as a positive control in the cerebellum on the right side, staining of the Purkinje cells (*arrows*). *Scale bar*=500 μm (*above*) and 70 μm (*below*)

KCTD7 Localizes to the Perinuclear Region in Transfection Experiments

We expressed the recombinant KCTD7 protein in COS-7 cells, tagged with either GFP, HIS or HA and used immunofluorescence to detect the protein by fluorescence microscopy as shown in Fig. 2d. GFP-KCTD7 was detected with a specific GFP antibody, while HIS-KCTD7 and HA-KCTD7 were detected using either HIS or HA antibodies or with anti-KCTD7 antibodies. KCTD7 was found in the cytoplasm, with the highest expression close to the nucleus. Expression at the plasma membrane was very faint or absent. Additional confocal microscopy using anti-KCTD7 antibodies (Abcam) on COS-7 cells expressing HIS-KCTD7 confirmed the cytosolic expression, with a stronger but not specific perinuclear signal as shown in Fig. 2e.

KCTD7 is Able to Homodimerize and to Associate with Cullin-3

We co-transfected two tagged KCTD7 constructs, HIS-KCTD7 and HA-KCTD7, in COS-7 cells. After cell lysis, protein samples were purified on G-sepharose beads coupled with specific anti-HIS tag or anti-HA tag antibodies. Purified samples were then analyzed by Western blotting and KCTD7 proteins were detected using HA tag or HIS tag antibodies, respectively. As show in Fig. 4b, HA-KCTD7 was purified by co-immunoprecipitation when G-sepharose beads were coupled with the HIS tag antibody, and similarly HIS-KCTD7 was purified when G-sepharose beads were coupled with the HA tag antibody. These data indicate that KCTD7 is able to homodimerize or multimerize into a higher order protein complex.

We then tested the ability of KCTD7 to bind Cullin1 or Cullin-3. We co-transfected COS-7 cells with KCTD7 and HA-CUL1 or HA-CUL3-tagged constructs. Cells were lysed 48 h after transfection, and protein samples were purified on G-sepharose beads coupled with either anti-KCTD7 or anti-HA antibody. The purified samples were then analyzed by Western blotting using KCTD7 or HA tag antibodies (Fig. 4c). The results showed that KCTD7 was able to co-immunoprecipitate with CUL3 but not with CUL1. Cross-experiments showed that CUL3 was able to co-immunoprecipitate with KCTD7 but CUL1 was not.

This specific interaction with CUL3 suggested that KCTD7 could be part of an E3 ubiquitin ligase multi-protein complex. Such a complex is involved in the ubiquitination of proteins which are subsequently degraded by the proteasome. To assess whether KCTD7 itself could be subject to ubiquitination, we co-transfected KCTD7 and Flag-ubiquitin in COS-7 cells and purified protein samples on G-Sepharose beads coupled with an anti-Flag antibody. The purified ubiquitinated proteins were then analyzed by Western blotting using the KCTD7-antibody (Abnova). As shown in Fig. 4d, no KCTD7 was found to be ubiquitinated.

Discussion

We showed that KCTD7 overexpression in transfected primary cultures of murine neurons resulted in hyperpolarization of the resting membrane potential and decreased their excitability in patch clamp experiments. Therefore, a genetic defect causing the loss of KCTD7 expression, as a result of a biallelic nonsense mutation observed in our previously reported patients, is consistent with a depolarized resting membrane potential and increased excitability, and hence with an epileptic phenotype.

KCTD7 mRNA in situ hybridization and protein immunohistochemistry in murine brain slices produced completely superimposable images showing a strongest KCTD7 expression in the mitral cells of the olfactory bulb, the hippocampal gyrus dentate and CA1-CA3 cells, the deep layers of the cerebral cortex and the Purkinje cells of the cerebellum. This expression pattern is consistent with a mouse model of PME. Indeed, the Cstb −/− mouse is a model for the human CSTB defect, or Unverricht-Lundborg disease (EPM1; OMIM254800), an inherited neurodegenerative disease transmitted as an autosomal recessive trait which is the most common single known cause of PME worldwide [11]. The Cstb −/− mice develop myoclonic seizures and progressive ataxia, as observed in EPM1 [12] and in our previously reported patients with the KCTD7 defect. Young Cstb −/− mice (3–4 months old) display increased apoptosis in the cerebellar granular cell neurons, the hippocampal formation and the entorhinal cortex. Older mutant mice (16–18 months old) show gliosis of the neocortex and striatum, as well as of the entorhinal cortex and hippocampal formation. These secondary changes are very consistent with a primary neurodegenerative disorder that selectively targets specific cells.

Among the PME patients with the KCTD7 defect, the more severely affected also presented the most intractable myoclonus, and their neurological condition was improved when epilepsy was better controlled with AEDs, which suggests that the epileptic disorder itself played a role in the neurological deterioration. Such a disease progression is observed in Dravet syndrome patients, in whom the occurrence of convulsive status epilepticus episodes is the rule and is believed to contribute to the cognitive decline [13]. Dravet syndrome has been associated with mutations in the alpha subunit of the voltage-gated sodium channel Nav1.1 (SCN1A), both in sporadic and familial cases (Claes et al. 2001; [14]). Clearly our patients' disease cannot be diagnosed as Dravet syndrome because the onset of seizures was after the age of 1 year and because of the absence of convulsive seizures in two out of the three

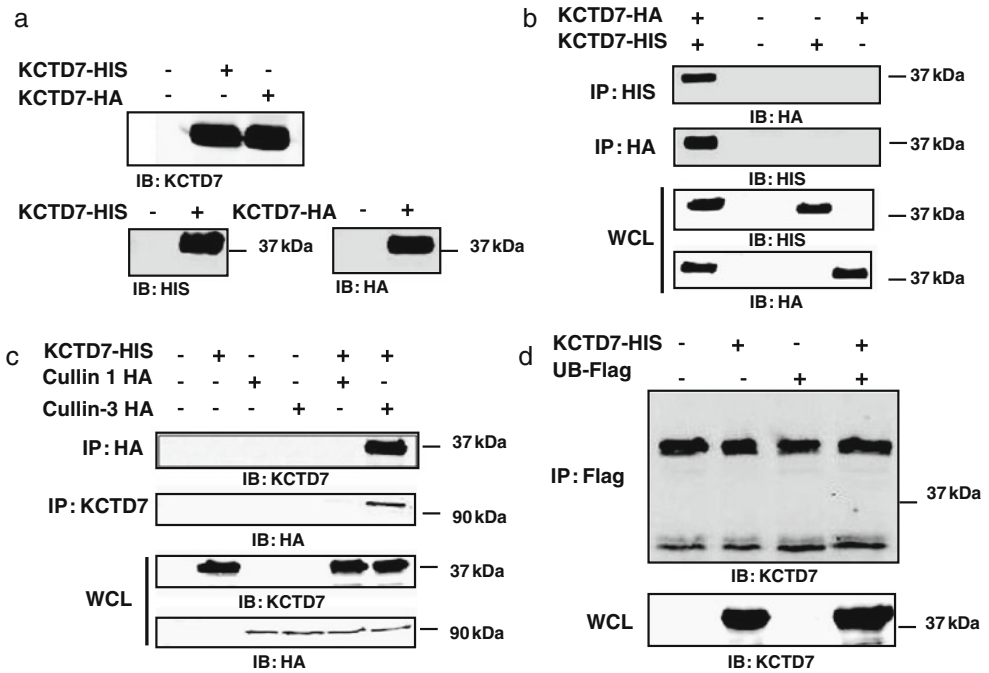

Fig. 4 Co-immunoprecipitation assays. **a** Antibodies used during immnunodetections were tested for their specificity. HIS-KCTD7- and HA-KCTD7-overexpressed samples were detected using both KCTD7 and the tag antibodies. **b** COS-7 cells were transiently transfected with KCTD7-HA, KCTD7-HIS or both. The expression of both constructs was revealed by immunoblot [whole cell lysis (*WCL*)]. Anti-HA or anti-HIS immunoprecipitates were, respectively, immunoblotted with anti-HIS or anti-HA antibobies. **c** Protein extracts from COS-7 cells transiently transfected with KCTD7 alone, or in combination with Cullin1-HA or Cullin-3-HA were immunoblotted with anti-KCTD7 or with anti-HA antibodies to ensure expression of the constructs (*WCL*). Proteins were immunoprecipitated by HA- or specific KCTD7 antibodies (*IP*) and revealed by immunoblotting (*IB*) using antibodies as indicated. **d** COS-7 cells were co-transfected with KCTD7 and/or Flag-ubiquitin constructs. Protein extracts were immunoprecipitated using anti-Flag antibodies and the precipitate revealed with KCTD7-specific antibodies

patients [15]. However, the occurrence of clinical regression early in the course of the disease, the fluctuation of the disease with epilepsy control by anti-epileptic drugs, and the presence of myoclonus are clinical similarities. Our observations thus suggest that a genetic defect of the resting potential and excitability in neurons was the primary cause of PME in our patients, and that its progression resulted at least in part from the severity of the epilepsy itself.

The membrane potential depends on several factors that include the concentration of ions across the membrane, the activity of the Na+/K+ ATPase in the plasma membrane, and the permeability of ion channels. Potassium has the highest permeability across the membrane, and in physiological conditions, the distribution of potassium ions is the most important factor that determines the resting membrane potential. Indeed, the resting potential is close to the equilibrium potential predicted from K+ concentrations across the membrane by the Nernst equation. With some small permeability to other ions (mainly Na+) that depolarize the membrane, the resting potential is almost always smaller (less negative) than expected by the Nernst equation. Potassium channels like the inwardly rectifying potassium channel (Kir) compensate by allowing K+ outward, thereby repolarizing the membrane [16]. We hypothesized that KCTD7 is required for the proper permeability of such a non-gated potassium channel that functions in a voltage range around the resting potential, which is consistent with the increased electrical conductance observed in KCTD7-transfected neurons.

Four KCTD proteins, each with a distinct expression profile in the brain (KCTD8, 12, 12b and 16) have recently been shown to associate as auxiliary subunits with GABAb receptor subunits in order to produce co-assembled GABAb receptors with modified G protein-signaling properties [17]. G protein signaling, in turn, controls potassium conductance via the inward Kir channels [18]. The hypothesis of a direct effect of KCTD7 at the plasma membrane, either with a G protein-coupled receptor or with a potassium channel was, however, not supported by the immunofluorescence of transfected KCTD7 in COS-7 cells, which showed cytoplasmic expression of the recombinant protein, with a stronger perinuclear signal, and absent or very faint expression at the membrane.

We showed by co-immunoprecipitation experiments that KCTD7 is able to homodimerize (Fig. 4a) and to bind CUL3, but not CUL1 (Fig. 4b). We also showed that KCTD7 was not itself ubiquitinated (Fig. 4c). KCTD5 has

been shown to multimerize in solution, and to function as an adaptor for CUL3 [19], allowing for CUL3 substrates to become ubiquitinated. Like KCTD7, it is interesting to notice that the KCTD5 protein is specifically expressed while its mRNA is ubiquitous. Therefore, we can speculate that the KCTD7 mRNA is present in most tissues but inactivated by a miRNA-mediated control regulating the protein synthesis. KCTD11 was shown to associate with Cullin-3 to form a functional E3 ubiquitin ligase that in turn drives the degradation of histone deacetylase HDAC1 [9]. Therefore, we made the hypothesis that KCTD7-induced proteasome degradation of some yet unidentified substrate might directly or indirectly increase potassium conductance at the cell membrane. Alternatively, ubiquitination might modify the activity, function or localization of its substrate, allowing the speculation that KCTD7 might directly increase the conductance of a non-gated potassium channel. However, as the precise molecular mechanisms linking KCTD7 with Cullin-3 and the effect on the membrane potential could not be resolved, it would be very interesting to consider additional electrophysiological measures on cortical neurones overexpressing either Cullin-3 alone or both KCTD7 and Cullin-3 and compare the electrophysiological profiles under these conditions to our previous data.

Of note, the voltage-gated potassium channels KCNQ2/3 and KCNQ3/5 were shown to be regulated by ubiquitination [20] this effect being mediated by the Nedd4-2 ubiquitin ligases. Other studies have shown that voltage-gated potassium channels Kv1.3 [21] and 1.5 [22], the current rectifier potassium channel KCNH2 [23], as well as the voltage-gated sodium channels Nav1.2, Nav1.7 and Nav1.8 [24], and the chloride channels CIV-5 [25], TTYH2 and TTYH3 [26] are all regulated by a plasmic membrane expression control conducted by the Nedd4-5 ubiquitin ligase. These very interesting data show that the ubiquitination of transmembrane ion channels is a regulation mechanism of their cell membrane expression frequently observed.

Another study on actinfilin [27], a BTB/POZ protein highly expressed in nervous tissues, showed that it is able to bind Cullin-3 to mediate the ubiquitination of the kainate receptor subunit GluR6. It is known that kainate, a neurotoxic analog of glutamate, has been implicated in frontal lobe epilepsy models [28]. Fisahn et al. [29] showed by patch clamp measurements on wild type and GluR6 −/− hippocampal CA1 and CA3 pyramidal neurons that the absence of GluR6 induces a loss of ionotropic synaptic transmission and the loss of the post-hyperpolarization potassium currents (I_{sAHP} et I_{mAHP}) inhibition, leading to an increase of the cell membrane excitability. These data help us to speculate a potential role of KCTD7 and Cullin-3 in the cell membrane excitability modulation. In summary, we show that KCTD7 increases the potassium conductance at the plasma membrane of transfected neurons, either directly or indirectly, consistent with an epileptogenic effect of the genetic KCTD7 defect as observed in our patients with a biallelic null mutation of the *KCTD7* gene and inherited PME.

Acknowledgments Regis Azizieh is a PhD student supported by the FRIA (Fonds pour la formation à la Recherche dans l'Industrie et dans l'Agriculture) and Van Buuren grants. Marc J. Abramowicz and Serge N. Schiffmann are supported by FRSM (Fonds de la Recherche scientifique médicale) grants of the Belgian FNRS (Fonds national de la Recherche Scientifique), Marc J. Abramowicz is supported by the Fonds Erasme and Serge N. Schiffmann by grant from the Queen Elisabeth Medical foundation (FMRE, Belgium). We thank Pierre Vanderhaeghen and Alban de Kerchove d'Exaerde for discussion and Sandra Strollo, Chantal Degraef, Patrick Massoma and Sandra Pietri for expert technical help.

References

1. Stogios PJ, Downs GS, Jauhal JJ, Nandra SK, Prive GG (2005) Sequence and structural analysis of BTB domain proteins. Genome Biol 6:R82
2. Azizieh R, Van Bogaert P, Désir J, Aeby A, De Meirleir L, Laes JF, Christiaens F, Abramowicz MJ (2007) Mutation of a potassium channel-related gene in progressive myoclonic epilepsy. Ann Neurol 61(6):579–586
3. Niedermeyer E, Lopes Da Silva F (2005) Electroencephalography: basic principles, clinical applications, and related fields. Lippicott Williams & Wilkins, Philadelphia, p 389
4. Singh NA, Charlier C, Stauffer D, DuPont BR, Leach RJ, Melis R, Ronen GM, Bjerre I, Quattlebaum T, Murphy JV, McHarg ML, Gagnon D, Rosales TO, Peiffer A, Anderson VE, Leppert M (1998) A novel potassium channel gene, KCNQ2, is mutated in an inherited epilepsy of newborns. Nat Genet 18(1):25–29
5. Charlier C, Singh NA, Ryan SG, Lewis TB, Reus BE, Leach RJ, Leppert M (1998) A pore mutation in a novel KQT-like potassium channel gene in an idiopathic epilepsy family. Nat Genet 18 (1):53–55
6. Ota T, Suzuki Y, Nishikawa T, Otsuki T, Sugiyama T, Irie R, Wakamatsu A, Hayashi K, Sato H, Nagai K, Kimura K, Makita H, Sekine M, Obayashi M, Nishi T, Shibahara T, Tanaka T, Ishii S, Yamamoto J, Saito K, Kawai Y, Isono Y, Nakamura Y, Nagahari K, Murakami K, Yasuda T, Iwayanagi T, Wagatsuma M, Shiratori A, Sudo H, Hosoiri T, Kaku Y, Kodaira H, Kondo H, Sugawara M, Takahashi M, Kanda K, Yokoi T, Furuya T, Kikkawa E, Omura Y, Abe K, Kamihara K, Katsuta N, Sato K, Tanikawa M, Yamazaki M, Ninomiya K, Ishibashi T, Yamashita H, Murakawa K, Fujimori K, Tanai H, Kimata M, Watanabe M, Hiraoka S, Chiba Y, Ishida S, Ono Y, Takiguchi S, Watanabe S, Yosida M, Hotuta T, Kusano J, Kanehori K, Takahashi-Fujii A, Hara H, Tanase TO, Nomura Y, Togiya S, Komai F, Hara R, Takeuchi K, Arita M, Imose N, Musashino K, Yuuki H, Oshima A, Sasaki N, Aotsuka S, Yoshikawa Y, Matsunawa H, Ichihara T, Shiohata N, Sano S, Moriya S, Momiyama H, Satoh N, Takami S, Terashima Y, Suzuki O, Nakagawa S, Senoh A, Mizoguchi H, Goto Y, Shimizu F, Wakebe H, Hishigaki H, Watanabe T, Sugiyama A, Takemoto M, Kawakami B, Yamazaki M, Watanabe K, Kumagai A, Itakura S, Fukuzumi Y, Fujimori Y, Komiyama M, Tashiro H, Tanigami A, Fujiwara T, Ono T, Yamada K, Fujii Y, Ozaki K, Hirao M, Ohmori Y, Kawabata A, Hikiji T, Kobatake N, Inagaki H, Ikema Y, Okamoto S, Okitani R, Kawakami T, Noguchi S, Itoh T, Shigeta K, Senba T, Matsumura K, Nakajima Y, Mizuno T, Morinaga M,

Sasaki M, Togashi T, Oyama M, Hata H, Watanabe M, Komatsu T, Mizushima-Sugano J, Satoh T, Shirai Y, Takahashi Y, Nakagawa K, Okumura K, Nagase T, Nomura N, Kikuchi H, Masuho Y, Yamashita R, Nakai K, Yada T, Nakamura Y, Ohara O, Isogai T, Sugano S (2004) Complete sequencing and characterization of 21,243 full-length human cDNAs. Nat Genet 36(1):40–45

7. NCBI Reference Sequence: NC_000007.13
8. Dutta S, Dawid IB (2010) Kctd15 inhibits neural crest formation by attenuating Wnt/beta-catenin signaling output. Development 137(18):3013–3018, Epub 2010 Aug 4
9. Canettieri G, Di Marcotullio L, Greco A, Coni S, Antonucci L, Infante P, Pietrosanti L, De Smaele E, Ferretti E, Miele E, Pelloni M, De Simone G, Pedone EM, Gallinari P, Giorgi A, Steinkühler C, Vitagliano L, Pedone C, Schinin ME, Screpanti I, Gulino A (2010) Histone deacetylase and Cullin-3-REN (KCTD11) ubiquitin ligase interplay regulates Hedgehog signalling through Gli acetylation. Nat Cell Biol 12(2):132–142, Epub 2010 Jan 17
10. D'Angelo E, De Filippi G, Rossi P, Taglietti V (1995) Synaptic excitation of individual rat cerebellar granule cells in situ: evidence for the role of NMDA receptors. J Physiol 484(Pt 2):397–413
11. Joensuu T, Kuronen M, Alakurtti K, Tegelberg S, Hakala P, Aalto A, Huopaniemi L, Aula N, Michellucci R, Eriksson K, Lehesjoki A-E (2007) Cystatin B: mutation detection, alternative splicing and expression in progressive myoclonus epilepsy of Unverricht-Lundborg type (EPM1) patients. Eur J Hum Genet 15:185–193
12. Pennacchio LA, Bouley DM, Higgins KM, Scott MP, Noebels JL, Myers RM (1998) Progressive ataxia, myoclonic epilepsy and cerebellar apoptosis in cystatin B-deficient mice. Nat Genet 20 (3):251–258
13. Fujiwara T (2006) Clinical spectrum of mutations in SCN1A gene: severe myoclonic epilepsy in infancy and related epilepsies. Epilepsy Res 70(Suppl 1):S223–S230, Epub 2006 Jun 27
14. Nabbout R, Gennaro E, Dalla Bernardina B, Dulac O, Madia F, Bertini E, Capovilla G, Chiron C, Cristofori G, Elia M, Fontana E, Gaggero R, Granata T, Guerrini R, Loi M, La Selva L, Lispi ML, Matricardi A, Romeo A, Tzolas V, Valseriati D, Veggiotti P, Vigevano F, Vallée L, Dagna Bricarelli F, Bianchi A, Zara F (2003) Spectrum of SCN1A mutations in severe myoclonic epilepsy of infancy. Neurology 60(12):1961–1967
15. Escayg, Goldin (2010) Epilepsia 51:1650–1658
16. Benatar M (2000) Neurological potassium channelopathies. QJM 93(12):787–797
17. Schwenk J, Metz M, Zolles G, Turecek R, Fritzius T, Bildl W, Tarusawa E, Kulik A, Unger A, Ivankova K, Seddik R, Tiao JY, Rajalu M, Trojanova J, Rohde V, Gassmann M, Schulte U, Fakler B, Bettler B (2010) Native GABAb receptors are heteromultimers with a family of auxiliary subunits. Nature 465(7295):231–235. doi:10.1038/nature08964
18. Yi BA, Minor DL Jr, Lin YF, Jan YN, Jan LY (2001) Controlling potassium channel activities: interplay between the membrane and intracellular factors. Proc Natl Acad Sci USA 98(20):11016–11023
19. Bayón Y, Trinidad AG, de la Puerta ML, Del Carmen Rodríguez M, Bogetz J, Rojas A, De Pereda JM, Rahmouni S, Williams S, Matsuzawa S, Reed JC, Crespo MS, Mustelin T, Alonso A (2008) KCTD5, a putative substrate adaptor for Cullin-3 ubiquitin ligases. FEBS J 275(15):3900–3910, EpubJun 28
20. Ekberg J, Schuetz F, Boase NA, Conroy SJ, Manning J, Kumar S, Poronnik P, Adams DJ (2007) Regulation of the voltage-gated K (+) channels KCNQ2/3 and KCNQ3/5 by ubiquitination. Novel role for Nedd4-2. J Biol Chem 282(16):12135–12142
21. Henke G et al (2004) Regulation of the voltage gated K+ channel Kv1.3 by the ubiquitin ligase Nedd4-2 and the serum and glucocorticoid inducible kinase SGK1. J Cell Physiol 199 (2):194–199
22. Boehmer C et al (2008) Modulation of the Voltage-Gated Potassium Channel Kv1.5 by the SGK1 Protein Kinase Involves Inhibition of Channel Ubiquitination. Cell Physiol Biochem 22(5–6):591–600
23. Chapman H et al (2005) Downregulation of the HERG (KCNH2) K^+ channel by ceramide: evidence for ubiquitin-mediated lysosomal degradation. J Cell Sci 118(22):5325–34
24. Fotia AB et al (2004) Regulation of neuronal voltage-gated sodium channels by the ubiquitin-protein ligases Nedd4 and Nedd4–2. J Biol Chem 279(28):28930–5
25. Hryciw DH et al (2004) Nedd4–2 functionally interacts with ClC-5: involvement in constitutive albumin endocytosis in proximal tubule cells. J Biol Chem 279(53):54996–5007
26. He Y et al (2008) The ubiquitin-protein ligase Nedd4–2 differentially interacts with and regulates members of the Tweety family of chloride ion channels. J Biol Chem 283(35):24000–10
27. Salinas GD, Blair LA, Needleman LA, Gonzales JD, Chen Y, Li M, Singer JD, Marshall J (2006) Actinfilin is a Cul3 substrate adaptor, linking GluR6 kainate receptor subunits to the ubiquitin-proteasome pathway. J Biol Chem 281(52):40164–40173
28. Nadler JV (1981) Kainic acid as a tool for the study of temporal lobe epilepsy. Life Sci 29(20):2031–2042
29. Fisahn A, Heinemann SF, McBain CJ (2005) The kainate receptor subunit GluR6 mediates metabotropic regulation of the slow and medium AHP currents in mouse hippocampal neurones. J Physiol 562(1):199–203